# Activity Induced Rigidity of Liquid Droplets

Kaili Xie, Benjamin Gorin, Rory Cerbus, Laura Alvarez, Jean-Michel Rampnoux, Hamid Kellay

# Activity Induced Rigidity of Liquid Droplets

Kaili Xie,[1] Benjamin Gorin,[1] Rory T. Cerbus,[1] Laura Alvarez,[2]
Jean-Michel Rampnoux,[1] and Hamid Kellay[1,3,*]
[1]Université de Bordeaux, CNRS, LOMA, UMR 5798, F-33405 Talence, France
[2]Université de Bordeaux, CNRS, CRPP, UMR 5031, 33600 Pessac, France
[3]Institut Universitaire de France, 75005 Paris, France

(Received 8 December 2021; revised 18 February 2022; accepted 25 August 2022; published 21 September 2022)

Here we show that encapsulating active Janus particles within a drop renders it more resistant to deformation. This drop is deformed under the action of an extensional flow. Such deformation is primarily resisted by the drop interfacial tension. When the particles are active under the action of laser illumination, the deformation decreases signaling an increase in effective tension or Laplace pressure. This increase is attributed to the activity of the particles. Our results using numerous drop sizes, particle number densities, and active velocities show that the obtained increase agrees surprisingly well, over an extended range, with a standard expression for the pressure engendered by an ensemble of active particles, proposed years ago but not tested yet in three dimensions.

DOI: 10.1103/PhysRevLett.129.138001

The pressure of an ensemble of active particles is a fundamental but much debated property [1–8]. Whether an equation of state relating pressure to number density exists for the different families of active particles, how this pressure depends on particle-particle interactions and on particle interactions with surrounding walls, or what is the role of geometry and wall curvature are typical questions [7,9–11]. Establishing the dependence of the mechanical pressure of active systems on system parameters permits the exploration of different perspectives in active matter, notably self-assembly, phase separation, and encapsulation [1,12,13].

Recent theoretical work has established the conditions under which an equation of state and thus a relation between pressure and density can be obtained: For noninteracting particles with negligible particle wall and interparticle torques, it is generally accepted that this pressure is a function of not only the number density of the particles but also their velocity and persistence time [7,14]. The existence of an equation of state is however valid in exceptional cases only. Recent experiments showing this exceptional character have been carried out using a two-dimensional layer of millimeter-sized self-propelled particles [9]. On the other hand, experimental work on two-dimensional chemically propelled micrometer-sized particles did show that an equation of state can be obtained [15]. Most experimental studies so far focus on the two-dimensional case, and few if any address the issue in three-dimensional situations.

These considerations bring us to the core subject of this Letter which concerns the effects of an active system on confining boundaries in three dimensions. For this purpose, we propose a simple experiment based on the deformation of a drop filled with active particles and subjected to an extensional flow field. Our main observation is that activity engenders an additional resistance of the drop toward deformation. Active particles have been encapsulated in vesicles or flexible containers before mostly to examine deformation modes or global mobility [2,13,16–18].

Drop deformation in an extensional flow was studied almost a century ago by Taylor and later revisited by different studies [19–21]. In such a controlled flow [22], the drop deforms to become elliptical. The deformation of the drop is given analytically by an expression where the viscosity ratio between inner drop and outer fluid plays a minor role [19,23]. The major role is played by the extensional rate, fixed and controlled experimentally, which drives the drop deformation and the Laplace pressure which resists deformation. Here, when the drop is filled with active particles, i.e., spherical Janus particles driven by light, the measured deformation decreases indicating a higher effective surface tension or Laplace pressure. This excess mechanical pressure, which we have measured using different active particle velocities, number densities, and particle sizes, turns out to be well described by an expression for the pressure of an assembly of active particles, introduced in different studies [1–3,5–7], over an extended range of parameters. Considering that our system includes hydrodynamic interactions and that the existence of an equation of state is the exception rather than the norm, our results are both surprising and unexpected.

Our active particles are Janus microparticles driven by light [24–26] with nominal radii ranging from 1.3 $\mu$m to 10 $\mu$m made of poly(methyl methacrylate) (PMMA) or polystyrene (PS). These particles were half coated with a layer of titanium which absorbs light to render them active.

 

To increase adhesion of this titanium layer on the particle surface, a 10 nm thick layer of chromium was precoated on one half of the particles, prior to deposition of the 50 nm titanium layer (see the Supplemental Material, Fig. S1 [27]). The prepared Janus particles were then washed several times with ethanol and deionized water and dried in an oven (Memmert Model 400) at 35 °C for several days before further use. A suspension of active particles with the desired volume fraction (0.5%–10%) was prepared by suspending the Janus particles in an aqueous mixture of deionized water (50 wt%), 2-pyridinemethanol (40 wt%), and glycerol (10 wt%) to achieve density matching. Dextran (15 wt%, average molecular weight 64 000) was used to increase the viscosity of the aqueous phase with the solution remaining Newtonian. To achieve low interfacial tension and avoid particle aggregation, sodium bis(2-ethylhexyl) sulfosuccinate with a cosurfactant cetyltrimethylammonium bromide was added to the aqueous solution [28,29]. Suspensions of passive particles (PMMA or PS) without metallic coating were also prepared in the same way and used at concentrations similar to the active suspensions to directly test the effect of activity.

Particle suspensions were then encapsulated in the drops via water-in-oil emulsification in silicone oil (AR1000, Wacker Chemie AG). The density difference between the drop phase and the oil phase is less than 0.01 g/mL; thus sedimentation and buoyancy are negligible. Both the active and passive particles show no specific interactions with the drop interface in the prepared emulsions without laser illumination (see the Supplemental Material, Videos S1 and S2 [27]). Janus or passive particle laden droplets were then deformed in a well-controlled extensional flow chamber [Fig. 1(a1)], described elsewhere [30,31]. Briefly, the droplets (diameter ranging from 65 $\mu$m to 160 $\mu$m) were trapped in the vicinity of the stagnation point ($v_x = v_y = v_z = 0$) in the symmetrical cross-slot chamber [27]. The extensional rate $\dot{\varepsilon}$ in experiments ranges from 0.15 $s^{-1}$ to 0.76 $s^{-1}$ was measured by a homemade Matlab particle tracking velocimetry technique [Fig. 1(a2) and the Supplemental Material, Fig. S2 [27] ]. The deviation of the extensional rate from its average value across the full observation window of 1200 $\mu$m × 1200 $\mu$m centered around the stagnation point is less than 5%. In the vertical direction, the extensional rate shows a parabolic profile as expected for a given flow rate. Correction of $\dot{\varepsilon}$ versus $z$ was taken into account with the known position of each drop in the $z$ direction (see the Supplemental Material [27]). The velocity field is planar and given by $[v_x, v_y, v_z] = [\dot{\varepsilon}x, -\dot{\varepsilon}y, 0]$, analogous to the four-roll mill configuration [19,21,23].

The normal stress balance across the interface gives rise to an axisymmetrical shape of the drop for small deformation with the major and minor lengths $L$ and $S$ in the plane of flow, respectively [23]. The deformation is defined as $D = (L - S)/(L + S)$. Figure 1(b) illustrates the dynamics

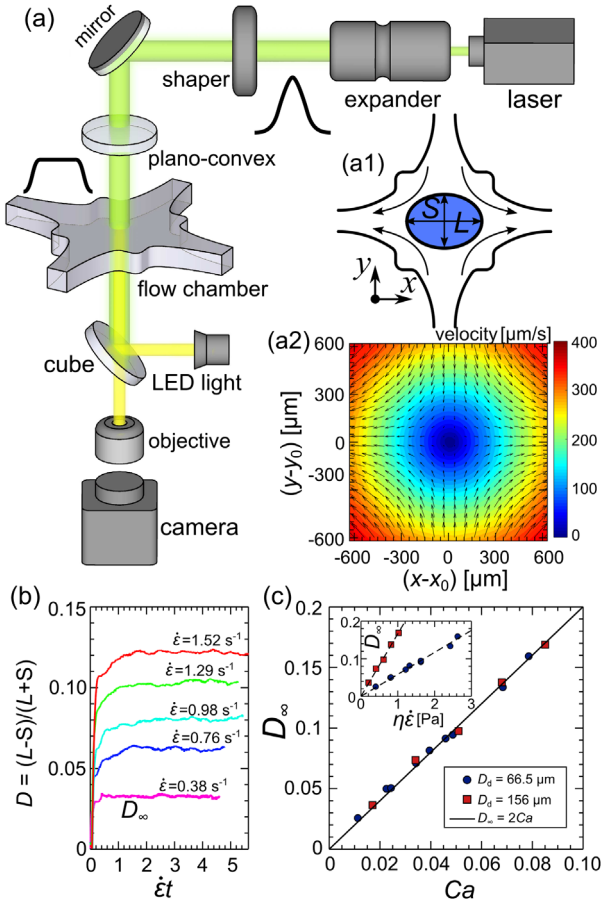


FIG. 1. Experiments. (a) Schematic of experimental setup. (a1) Sketch of extensional flow chamber with the deformed drop major and minor lengths $L$ and $S$. (a2) Flow field in the vicinity of the stagnation point $(x_0, y_0)$. (b) Drop deformation as a function of accumulated strain rate for various extensional rates. Drop diameter is 68.8 $\mu$m. (c) Steady-state deformation versus capillary number $Ca$. Solid line represents the small deformation theory [19]. Inset: steady-state deformation for two different drop sizes versus flow viscous stress.

of deformation of an individual drop versus the accumulated strain $\dot{\varepsilon}t$ for different extensional rates. The deformation reaches a plateau in a short time ($\dot{\varepsilon}t \leq 1$), the value of which gives the steady-state deformation $D_\infty$. Larger extensional rates lead to larger stable deformations $D_\infty$. The deviation of the drop shape from sphericity depends on both the viscous stress and the interfacial stress acting on the interface. Small deformation theory [19,20] gives the dependence of the steady-state deformation of a droplet in a linear extensional flow on the capillary number $Ca = \eta_s G/(\gamma/R)$ and the viscosity ratio $\lambda$,

$$D_\infty = 2Ca\frac{19\lambda + 16}{16\lambda + 16}, \tag{1}$$

where $R$ is the radius of the undeformed drop, $\gamma$ is the interfacial tension, and $G$ is equivalent to the shear strain

rate in the four-roll mill configuration [23,32,33]. In our experiments $G = \dot{\epsilon}/2$. The viscosity ratio $\lambda = \eta_d/\eta_s$ of the drop phase viscosity $\eta_d$ to the outer oil phase viscosity $\eta_s$ is much smaller than 1, so that $f(\lambda) = (19\lambda + 16)/(16\lambda + 16) \approx 1$. The deformation is dependent only on the extensional rate and the Laplace pressure. In the small deformation regime ($D_\infty \leq 10\%$), $D_\infty \approx 2Ca$, so that the interfacial tension $\gamma$ of the bare drops can be deduced with good precision [Fig. 1(c)]. Our measurements of the interfacial tension using this small deformation regime have been verified by an alternative measurement using a pendant drop [34] (Supplemental Material, Fig. S3 [27]): the agreement between the two methods is excellent.

Active particles were driven by asymmetric heating across the Janus particles using illumination from a top-hat laser beam (MSL532 300 mW, 532 nm wavelength). Specifically, the Gaussian laser profile is transformed into a homogeneous top-hat profile by a beam shaper (TOPAG FBSR-20-532) focused on the extensional plane where the drop deformation is monitored [Fig. 1(a)]. The homogeneously illuminated area has a diameter (from 90 to 160 $\mu$m) typically larger than the drop size so that all Janus particles are subjected to the same illumination (Supplemental Material, Fig. S5 [27]). Such top-hat profiles present no intensity gradients over the area occupied by the drops capable of generating optical forces. Further, the index of refraction mismatch between the two phases (drop phase $n = 1.428$ and oil phase $n = 1.460$) is small enough to minimize any alteration of the Laser beam profile due to its passage through the droplet. The drops and the particles were visualized using a camera (Orca Flash 4.0 from Hamamatsu) mounted on a microscope (Zeiss AXIO Observer). Light absorption at the metal-coated hemisphere produces a temperature gradient across the particle giving rise to its propulsion [35]. Figure 2 shows the Janus particles and their mobility for the different laser intensities. The particle velocity $u_p$, measured both within the drops and in a bulk solution, is approximately proportional to the laser intensity $I$, and the maximum speed can reach values as high as 100 $\mu$m/s which is generally difficult to achieve for Brownian particles [24]. While the particle velocity is sensitive to the solution viscosity, it is only mildly dependent on the particle size [Fig. 2(d)]. These Janus swimmers are observed to travel in straight lines, whether encapsulated in the drops or not, over relatively long distances [Figs. 2(b), 2(c), and the Supplemental Material, Fig. S6 [27] ] until they reach the surface of the drop when encapsulated, showing that our non-Brownian microswimmers are less prone to change direction compared with the Brownian ones.

Our principle result is shown in Fig. 3 which displays the deformation dynamics of a particle-filled drop exposed to laser illumination. The deformation $D$ is followed in time after the onset of the flow. This deformation, Fig. 3(b), starts out small and increases as time increases to settle on a

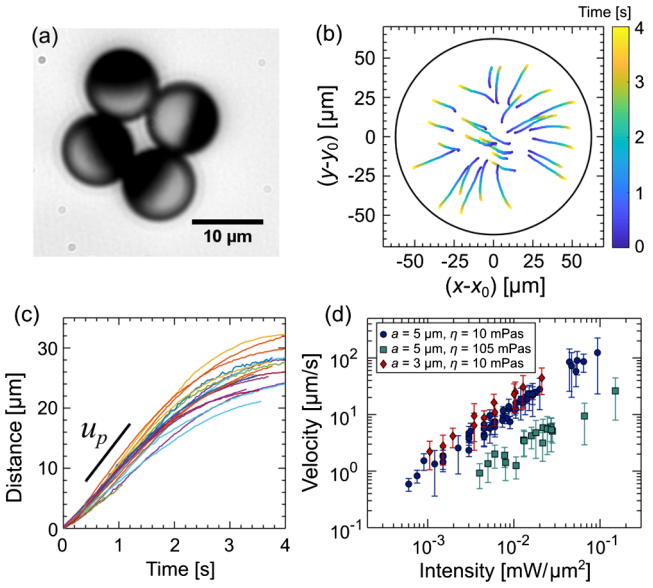


FIG. 2. Janus particles and their motility under laser illumination. (a) A bright field image of the Janus particles. The dark sides of the particles represent the metal coating. (b) Examples of the trajectories of active particles inside a static drop. The particles are polystyrene Janus ones with radius $a = 5$ $\mu$m. (c) Selected displacement versus time for the active particles shown in (b). (d) Velocity of active particles versus the laser intensity.

roughly constant value (steady-state deformation $D_\infty^{\max}$) when the flows inside and outside of the drop are well established. Particles slowly follow the streamlines of the internal flow. Once this plateau is reached, illumination is turned on while the drop remains near the stagnation point. Under illumination, the Janus particles move fast and eventually reach the drop surface [Fig. 3(a) and the Supplemental Material, Video S2 [27] ]. Tests using drops filled with passive particles under illumination show that they continue following the internal flow with no visible effect on the deformation of the droplet as shown in the inset of Fig. 3(b) (also see the Supplemental Material, Video S1 [27]). In the presence of Janus particles, the droplet deformation decreases strongly to settle on another smaller but roughly constant value $D_\infty^{\text{eff}}$ [Fig. 3(b)]. Since the laser illumination can increase the temperature of the fluid through heating the metal-coated particles, we have checked that this effect is not due to a surface tension variation with temperature. In fact, the surface tension decreases with an increase in temperature making this variation incompatible with a change in surface tension due to heating (Supplemental Material, Fig. S4 [27]).

The transition from large deformation to the smaller one due to activity takes roughly a few seconds, a timescale comparable with the mean time for Janus particles to reach the drop surface, depending on the particle velocity (Fig. S7 in the Supplemental Material [27]). When the laser illumination is turned off, the deformation goes back to its initial value, indicating that this effect is reversible and due to the activity of the Janus particles. Further, when the drop

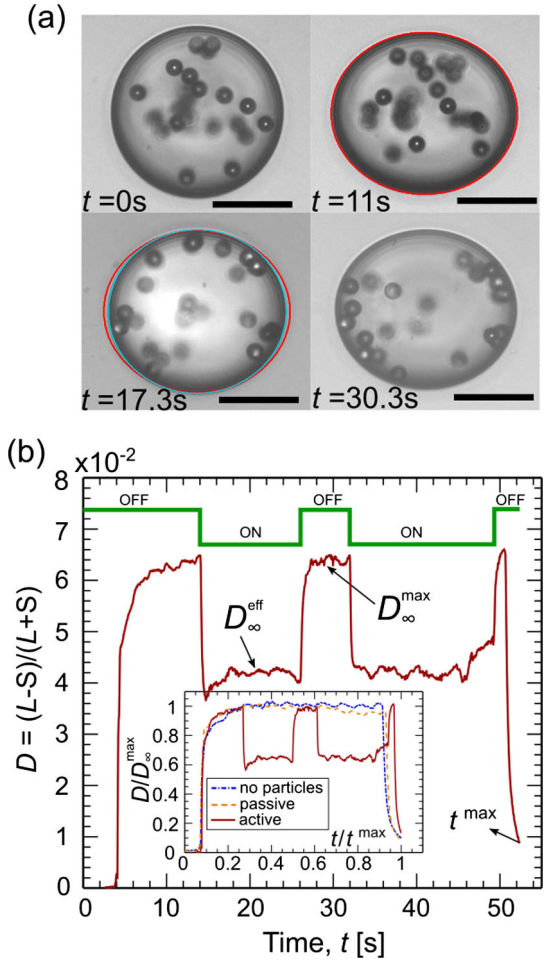


FIG. 3. Particle-filled drops and their deformation with laser off or on in the extensional flow. (a) Time-lapse images of the drop at different times. Red and light blue ellipses correspond to the drop at $t = 11$ s (in the absence of illumination) and $t = 17.3$ s (under illumination); see (b) for temporal evolution of the laser illumination and drop deformation. Scale bars, 40 $\mu$m. (b) Drop deformations under laser illumination off or on. The deformation decreases from its maximal value $D_\infty^{\max}$ to a value $D_\infty^{\text{eff}}$ under illumination. The green line shows when the laser is on or off. Inset: normalized deformation for particle-free, passive particles and active particles enclosed in drops versus time.

contains no particles or passive particles, the deformation remains the same [inset of Fig. 3(b)] with and without the laser illumination indicating that no optical forces are at play.

From such observations we conclude that the activity of the Janus particles engenders an additional stress to counterbalance the drop deformation. Since viscous effects contribute little to setting the deformation, the only possible effect is an additional mechanical pressure which should be additive with the inherent Laplace pressure $\gamma/R$. We thus represent the observed effect as an additional pressure [27],

$$P = \eta_s \dot{\varepsilon} \left( \frac{1}{D_\infty^{\text{eff}}} - \frac{1}{D_\infty^{\max}} \right), \tag{2}$$

where $D_\infty^{\text{eff}}$ and $D_\infty^{\max}$ are the stable deformations with and without laser illumination, respectively.

The values of the mechanical pressure $P$ extracted from the difference in the stable deformations is plotted in Fig. 4 for various experiments (see Table S1 in the Supplemental Material [27]) using different drop sizes, particle sizes, particle volume fractions (i.e., number densities), fluid viscosities, and laser illuminations (i.e., particle velocities). The pressure extracted from our measurements is insensitive to the extensional rate used (Fig. S8 in the Supplemental Material [27]), and has no systematic dependence on the radius of the drop thus ruling out curvature effects [10] (Figs. S9 and S10 in the Supplemental Material [27]). The type of surfactant and its concentration and thus the surface tension have little influence on the pressure (Fig. S11 in the Supplemental Material [27]). The pressure obtained is much higher than typical hydrodynamic stresses produced by the flow due to the particle's motion. The measured pressure increases with the number density and the velocity of Janus particles: this increase is consistent with a linear relation for number density and a quadratic dependence versus particle velocity. Such a dependence is surprisingly consistent with the pressure expression [Eq. (3)], already proposed in many studies of active particle assemblies [1–8]. The pressure of an ensemble of active particles can be written as

$$P = \frac{1}{6} n \zeta u_p^2 \tau_R, \tag{3}$$

where $n$ is the number density of active particles (swimmers), $\zeta = 6\pi\eta_d a$ is the mobility coefficient, $u_p$ is the velocity of the swimmers, and $\tau_R$ is the persistence or tumbling time of the active particles.

In order to test to what extent this expression describes our extensive results, we plot all of our data versus the expected pressure in Fig. 4(c). All of our experimental measurements collapse onto a single universal curve which is well approximated by the theoretical prediction [Eq. (3)] with the persistence time $\tau_R$ left as an adjustable parameter.

In this expression, when the mechanism for reorientation is due to thermal agitation, the value of $\tau_R = 1/D_R$, where $D_R$ is the rotational diffusion coefficient [1,7]. To collapse all the data in Fig. 4(c), we have used values of $\tau_R$ which depend on the viscosity of the inner fluid as well as the radius of the Janus particles. These values are shown in the inset of Fig. 4(c) and are in good agreement with the value of $1/D_R = 8\pi\eta_d a^3/k_B T$ with $k_B$ the Boltzmann constant and $T$ the temperature. There are small deviations of the collapsed data from the expected pressure mostly at high pressures which is also the high laser intensity zone. It is possible that a slight heating of the drop interior by the heated particles could be the cause of this deviation. Since both the surface tension and the viscosity of the liquid decrease with an increase in temperature (Supplemental Material, Fig. S4 [27]), they both

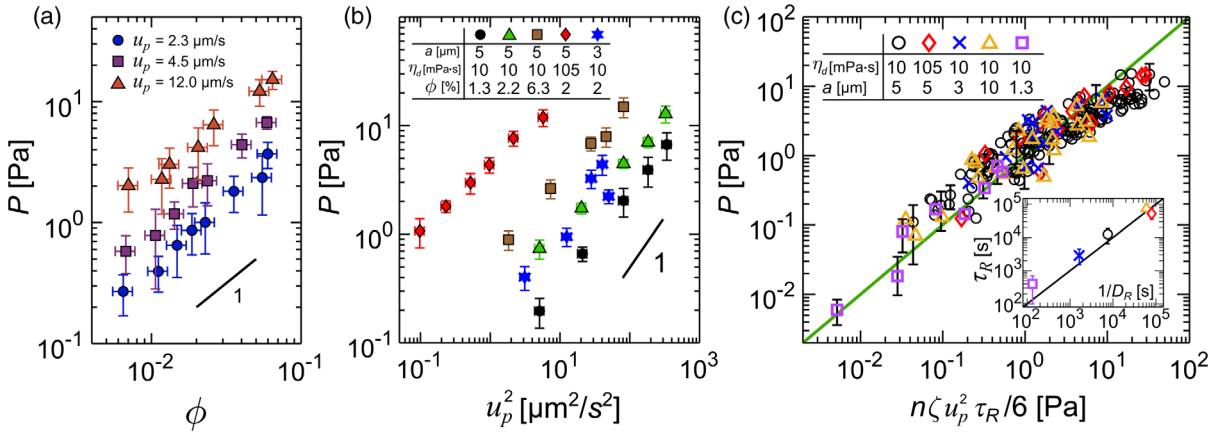


FIG. 4. Pressure. (a) Measured pressure versus active particle volume fraction $\phi$, for different self-propulsion velocities, where $\phi = n\frac{4}{3}\pi a^3$, $a$ is the particle radius, and $n$ corresponds to the particle number density. (b) Measured pressure versus the particle velocity squared. Different particle sizes, particle volume fractions, and fluid viscosities were tested. (c) Comparison of measured pressure with prediction of Eq. (3). Representative error bars are from the standard deviation using multiple measurements. Inset: active particle persistence time $\tau_R$ used in experiments versus the inverse of rotational diffusion constant $1/D_R$. Error bars correspond to the range of $\tau_R$ for which the collapse of the data in the main figure remain valid.

contribute to bring the experiments and the theoretical expression into accord. A decrease in surface tension, not accounted for in our measurements, would lead to underestimating the measured pressure, while a decrease of the viscosity (the theoretical expression for the pressure is proportional to the square of the viscosity) would lead to an overestimate of the theoretical pressure. From our estimates, and based on the variation of the surface tension and viscosity with temperature, a temperature rise of 3 K would bring the measured and expected pressures into good agreement (see Fig. S12 in the Supplemental Material).

To summarize, we have measured the mechanical resistance engendered by an assembly of active spherical and noninteracting particles to the deformation of a drop in which they are encapsulated. From a systematic study over an extended range of its dependence on active particle number density and particle velocity, as well as fluid and particle properties, it turns out that the measured mechanical resistance or pressure can be described by an expression for the pressure of an assembly of active particles proposed some years ago. Considering that hydrodynamic interactions are bound to play a role in the system used, this is both surprising and unexpected since an equation of state for active particles may exist only in a limited number of cases which require negligible particle wall and interparticle torques. A full analysis of the mechanical properties of this system including its hydrodynamics is an arduous theoretical task and is beyond the scope of this experimental work.

Nevertheless, the assemblies used here engender mechanical pressures as high as 10 Pa. These "high" mechanical pressures may have measurable repercussions on the properties of assemblies of particle laden droplets. We anticipate that an emulsion made of droplets encapsulating assemblies of active particles, i.e., an active emulsion, may show enhanced yield stress and possibly other effects related to the more rigid nature, due to activity, of the constituent droplets.

We thank the Institut Universitaire de France for financial support and LabEx AMADEUS ANR-10-LABEX-0042-AMADEUS Université de Bordeaux for partial financial support. R. T. C. gratefully acknowledges funding from the Horizon 2020 program under the Marie Skodowska-Curie Action Individual Fellowship (MSCAIF) (No. 793507). H. K. and J. M. R. would like to thank Aquitaine Region funding 2016 InMos (2016-1R60204-00007440). We thank Z. Shen for fruitful discussion, L. Healman and A. Tempel for help with flow chamber fabrication, and N. Kellay for help with some experiments.

*hamid.kellay@u-bordeaux.fr

[1] S. C. Takatori, W. Yan, and J. F. Brady, Swim Pressure: Stress Generation in Active Matter, Phys. Rev. Lett. **113**, 028103 (2014).

[2] M. Paoluzzi, R. Di Leonardo, M. C. Marchetti, and L. Angelani, Shape and displacement fluctuations in soft vesicles filled by active particles, Sci. Rep. **6**, 34146 (2016).

[3] M. C. Marchetti, J.-F. Joanny, S. Ramaswamy, T. B. Liverpool, J. Prost, M. Rao, and R. A. Simha, Hydrodynamics of soft active matter, Rev. Mod. Phys. **85**, 1143 (2013).

[4] X. Yang, M. L. Manning, and M. C. Marchetti, Aggregation and segregation of confined active particles, Soft Matter **10**, 6477 (2014).

[5] S. C. Takatori and J. F. Brady, Forces, stresses and the (thermo?) dynamics of active matter, Curr. Opin. Colloid Interface Sci. **21**, 24 (2016).

[6] F. Smallenburg and H. Löwen, Swim pressure on walls with curves and corners, Phys. Rev. E **92**, 032304 (2015).
[7] A. P. Solon, Y. Fily, A. Baskaran, M. E. Cates, Y. Kafri, M. Kardar, and J. Tailleur, Pressure is not a state function for generic active fluids, Nat. Phys. **11**, 673 (2015).
[8] W. Yan and J. F. Brady, The swim force as a body force, Soft Matter **11**, 6235 (2015).
[9] G. Junot, G. Briand, R. Ledesma-Alonso, and O. Dauchot, Active versus Passive Hard Disks against a Membrane: Mechanical Pressure and Instability, Phys. Rev. Lett. **119**, 028002 (2017).
[10] N. Nikola, A. P. Solon, Y. Kafri, M. Kardar, J. Tailleur, and R. Voituriez, Active Particles with Soft and Curved Walls: Equation of State, Ratchets, and Instabilities, Phys. Rev. Lett. **117**, 098001 (2016).
[11] S. C. Takatori and A. Sahu, Active Contact Forces Drive Nonequilibrium Fluctuations in Membrane Vesicles, Phys. Rev. Lett. **124**, 158102 (2020).
[12] S. C. Takatori and J. F. Brady, Swim stress, motion, and deformation of active matter: effect of an external field , Soft Matter **10**, 9433 (2014).
[13] H. R. Vutukuri, M. Hoore, C. Abaurrea-Velasco, L. van Buren, A. Dutto, T. Auth, D. A. Fedosov, G. Gompper, and J. Vermant, Active particles induce large shape deformations in giant lipid vesicles, Nature (London) **586**, 52 (2020).
[14] A. P. Solon, J. Stenhammar, R. Wittkowski, M. Kardar, Y. Kafri, M. E. Cates, and J. Tailleur, Pressure and Phase Equilibria in Interacting Active Brownian Spheres, Phys. Rev. Lett. **114**, 198301 (2015).
[15] F. Ginot, I. Theurkauff, D. Levis, C. Ybert, L. Bocquet, L. Berthier, and C. Cottin-Bizonne, Nonequilibrium Equation of State in Suspensions of Active Colloids, Phys. Rev. X **5**, 011004 (2015).
[16] A. Deblais, T. Barois, T. Guerin, P.-H. Delville, R. Vaudaine, J. S. Lintuvuori, J.-F. Boudet, J.-C. Baret, and H. Kellay, Boundaries Control Collective Dynamics of Inertial Self-Propelled Robots, Phys. Rev. Lett. **120**, 188002 (2018).
[17] J.-F. Boudet, J. Lintuvuori, C. Lacouture, T. Barois, A. Deblais, K. Xie, S. Cassagnere, B. Tregon, D. Brückner, J.-C. Baret *et al.*, From collections of independent, mindless robots to flexible, mobile, and directional superstructures, Sci. Rob. **6**, eabd0272 (2021).
[18] Y. Li and P. R. ten Wolde, Shape Transformations of Vesicles Induced by Swim Pressure, Phys. Rev. Lett. **123**, 148003 (2019).
[19] G. I. Taylor,The formation of emulsions in definable fields of flow, Proc. R. Soc. A **146**, 501 (1934).
[20] D. Barthes-Biesel and A. Acrivos, Deformation and burst of a liquid droplet freely suspended in a linear shear field, J. Fluid Mech. **61**, 1 (1973).
[21] B. J. Bentley and L. G. Leal, An experimental investigation of drop deformation and breakup in steady, two-dimensional linear flows, J. Fluid Mech. **167**, 241 (1986).
[22] S. J. Haward, M. S. N. Oliveira, M. A. Alves, and G. H. McKinley, Optimized Cross-Slot Flow Geometry for Microfluidic Extensional Rheometry, Phys. Rev. Lett. **109**, 128301 (2012).
[23] S. Kaur and L. G. Leal, Drop deformation and break-up in concentrated suspensions, J. Rheol. **54**, 981 (2010).
[24] I. Buttinoni, G. Volpe, F. Kümmel, G. Volpe, and C. Bechinger, Active Brownian motion tunable by light, J. Phys. Condens. Matter **24**, 284129 (2012).
[25] A. Würger, Self-Diffusiophoresis of Janus Particles in Near-Critical Mixtures, Phys. Rev. Lett. **115**, 188304 (2015).
[26] J. L. Moran and J. D. Posner, Phoretic Self-Propulsion, Annu. Rev. Fluid Mech. **49**, 511 (2017).
[27] See Supplemental Material at http://link.aps.org/supplemental/10.1103/PhysRevLett.129.138001 for experimental details and additional results.
[28] M. SinghaBakshi, Micelle formation by anionic and cationic surfactants in binary aqueous solvents, J. Chem. Soc., Faraday Trans. **89**, 4323 (1993).
[29] J. K. Hensel, A. P. Carpenter, R. K. Ciszewski, B. K. Schabes, C. T. Kittredge, F. G. Moore, and G. L. Richmond, Molecular characterization of water and surfactant AOT at nanoemulsion surfaces, Proc. Natl. Acad. Sci. U.S.A. **114**, 13351 (2017).
[30] V. Kantsler, E. Segre, and V. Steinberg, Critical Dynamics of Vesicle Stretching Transition in Elongational Flow, Phys. Rev. Lett. **101**, 048101 (2008).
[31] K. Xie, C. de Loubens, F. Dubreuil, D. Z. Gunes, M. Jaeger, and M. Leonetti, Interfacial rheological properties of self-assembling biopolymer microcapsules, Soft Matter **13**, 6208 (2017).
[32] L. G. Leal, Flow induced coalescence of drops in a viscous fluid, Phys. Fluids **16**, 1833 (2004).
[33] P. T. Corona, N. Ruocco, K. M. Weigandt, L. G. Leal, and M. E. Helgeson, Probing flow-induced nanostructure of complex fluids in arbitrary 2D flows using a fluidic four-roll mill (FFoRM), Sci. Rep. **8**, 1 (2018).
[34] F. Peters and D. Arabali, Interfacial tension between oil and water measured with a modified contour method, Colloids Surf. A **426**, 1 (2013).
[35] H.-R. Jiang, N. Yoshinaga, and M. Sano, Featured in Physics Editors' Suggestion Active Motion of a Janus Particle by Self-Thermophoresis in a Defocused Laser Beam, Phys. Rev. Lett. **105**, 268302 (2010).